Altitude distribution of electron concentration in ionospheric D-region in presence of time-varying solar radiation flux

A. Nina [a,*], V. Čadež [b], V. Srećković [a], D. Šulić [c]

[a] Institute of Physics, University of Belgrade, P.O. Box 57, Belgrade, Serbia
[b] Astronomical Observatory, Volgina 7, 11060 Belgrade, Serbia
[c] Faculty of Ecology and Environmental Protection, Union – Nikola Tesla University, Cara Dušana 62, 11000 Belgrade, Serbia

ABSTRACT

In this paper, we study the influence of solar flares on electron concentration in the terrestrial ionospheric D-region by analyzing the amplitude and phase time variations of very low frequency (VLF) radio waves emitted by DHO transmitter (Germany) and recorded by the AWESOME receiver in Belgrade (Serbia) in real time. The rise of photo-ionization rate in the ionospheric D-region is a typical consequence of solar flare activity as recorded by GOES-15 satellite for the event on March 24, 2011 between 12:01 UT and 12:11 UT. At altitudes around 70 km, the photo-ionization and recombination are the dominant electron gain and electron loss processes, respectively. We analyze the relative contribution of each of these two processes in the resulting electron concentration variation in perturbed ionosphere.

© 2011 Elsevier B.V. All rights reserved.

1. Introduction

Characteristics of the ionosphere and their changes are very important for life and human activity on the Earth. There are numerous studies about influences of ionospheric disturbances on operation of powerful energetic systems, navigation and remote radio communication systems, the atmospheric weather, the human health and the state of the entire biosphere [1,2]. Also, the earthquakes are recently recognized to induce perturbations in the lowest ionosphere that are registered as specific subionospheric VLF/LF transmitter signal anomalies (see [3] and references therein).

Methods of investigation of the ionospheric vertical structure are diverse depending on the applied measuring technics. At higher altitudes such as the F region (200–700 km), it is possible to perform direct measurements by probes and satellites while the lower ionosphere such as the D region (60–90 km) where the altitude range is too low for satellites and too high for atmospheric balloons, requires measurements mostly based on radio wave propagation techniques. The latter approach is the subject of this paper where we analyze and use the real time VLF signal recordings in recovering local plasma conditions in the D region. As the presence of electrons in the ionospheric D-region strongly affects the VLF radio wave propagation we present a method for determination of the electron concentration, its time derivative and vertical gradient profile in the D region. The method is based on recorded time variations of a chosen VLF signal when the ionospheric D region is perturbed by a solar flare. For such a case, we apply the analysis to two distinct regimes characterized by the electron concentration growing and decreasing in time that we further relate to the regimes with a dominant electron gain and loss process, respectively. The analysis of VLF signal in these two regimes yields conclusions on local plasma electron characteristics, chemical processes and dynamics in the D region. This method is analogous to the method of ionograms applied to the much higher F region by means of ionosondes [4].

As said, the structure and characteristics of the ionosphere are not constant, they vary in time depending on various external influences. In the sunlit part of the ionosphere, the most important affect comes from the solar activity which has been considered in many papers [5,6].

At altitudes about 70 km, the dominant electron gain and electron loss processes are the photo-ionization and recombination [7]. They are in equilibrium, i.e. mutually balanced, when the ionosphere is unperturbed. However, during periods of increased solar radiation, the rates of photo-ionization and recombination processes change in time and, consequently, so does the electron concentration.

In this work, we choose a typical X-ray solar flare recorded by the GOES-15 satellite on March 24, 2011 from 12:01 UT to 12:11 UT and we investigate the resulting perturbations induced in the ionosphere. Time and altitude dependent electron concentration

* Corresponding author.
  E-mail address: sandrast@ipb.ac.rs (A. Nina).

in the ionosphere is calculated by using the amplitude and phase variations of VLF signals emitted by the DHO (23.4 kHz) transmitter (Germany) that were registered by the Belgrade AWESOME receiver system (as a part of Stanford/AWESOME Collaboration for Global VLF Research) and numerically processed by the LWPC computing program [8] as done in [9,10].

2. Experimental data and calculation procedure

As of 12:03 UT, March 24, 2011, the Belgrade AWESOME VLF receiver recorded transient amplitude and phase increases for a signal at 23.4 kHz. Evidently, this was the consequence of a solar X-ray flare, class M1.0, registered by the GOES-15 satellite as can be seen in Fig. 1 showing time dependencies of solar flux (top panel) at wavelengths between 0.1 and 0.8 nm, and phase and amplitude time variations of the DHO signal (middle and bottom panel, respectively). The measurable features of the VLF signal refer to changes in amplitude ΔA_{rec} and phase ΔP_{rec} expressed in dB and degrees (both taken relative to the initial unperturbed state), respectively.

Our analysis of electron concentration is based on Wait's model of the ionosphere [11] which is characterized by two parameters: the wave reflection height $H'(t)$ and sharpness $\beta(t)$ used as input parameters for the LWPC computational procedure. The resulting computed changes of the VLF signal amplitude and phase are then compared with corresponding values of the registered wave which finally yields time dependent values for $H'(t)$ and $\beta(t)$ with resolution of 0.1 km and 0.001 km^{-1}, respectively.

The electron concentration $N(t,h)$ at time t and altitude h is calculated using the equation (from [11]):

$$N(t,h) = 1.43 \times 10^{13} e^{-\beta(t)H'(t)} e^{(\beta(t)-0.15)h}, \tag{1}$$

where the following units are assumed: $N(t,h)$ in m^{-3}, $\beta(t)$ in km^{-1}, and $H'(t)$ and h in km.

The above Eq. (1) exhibits the physical nature of the parameter $\beta(t)$ as a quantity related to some characteristic length $L(t)$ defined by $L(t) = 1/(\beta(t) - 0.15)$ km which is a typical e-folding distance for the electron spatial concentration decrease.

We are now interested in electron concentration in the D-region at the altitude of around 70 km. Time intervals with dominant photo-ionization and recombination processes are called the photo-ionization and recombination regime, respectively.

3. Results and discussion

Reflections of VLF waves occur at different heights H' depending on electron concentration. When a typical solar flare occurs, the total emitted radiation first increases in intensity and then falls off in the after-flare-maximum regime as given in Fig. 1, top panel. This causes corresponding changes in rates of photo-ionization and recombination processes which makes the electron concentration profile time dependent meaning that also the related VLF wave reflection height $H' = H'(t)$ and electron concentration gradient parameter $\beta = \beta(t)$ become functions of time t. Fig. 2 shows typical profiles $H'(t)$ and $\beta(t)$ resulting from the time varying radiation given in Fig. 1, top panel. We see that the wave reflecting height $H'(t)$ first decreases with time, reaches a minimum and starts rising afterwards. This can be explained by the fact that rise of radiation intensity increases the electron concentration at all heights which further results in steepening of the electron concentration gradient, i.e. growth of the parameter β, and lowering of the height H' at which the given frequency of the recorded VLF radio-wave becomes comparable with the local plasma frequency which itself is a function of electron concentration. Thus, an incident time-dependent radiation profile with a maximum in its intensity as given in Fig. 1 (top) causes a functional time-dependence $\beta(t)$ with a maximum and functional dependence $H'(t)$ with a minimum where both extrema occur at the same time t_m as seen in Fig. 2 and they are in a good agreement with values obtained by [9,12]. According to Eq. (1), two distinct time intervals $t \leqslant t_m$ and $t \geqslant t_m$ are related to the period of the electron concentration growth, and to that of electron concentration decrease, respectively (see
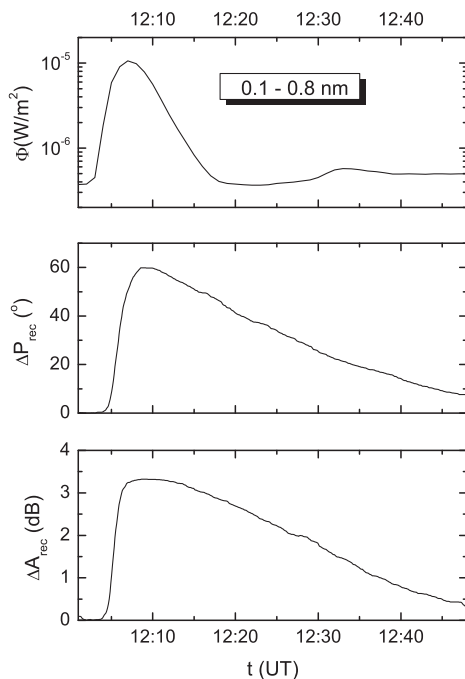

Fig. 1. Solar flux registered by GOES-15 satellite and phase and amplitude changes of signal emitted from DHO transmitter (Germany) and recorded on AWESOME receiver in Belgrade (Serbia) during observed flares. Zero values correspond to amplitude and phase recorded when ionosphere is non-perturbed.
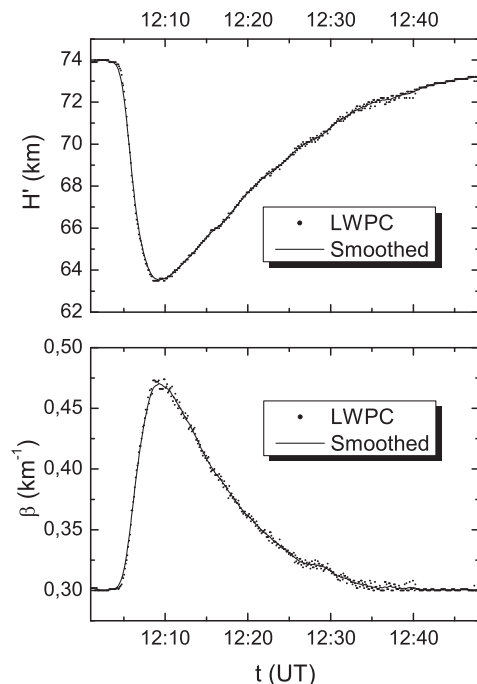

Fig. 2. The reflection height $H'(t)$ and sharpness $\beta(t)$ obtained by comparative LWPC simulation and recorded signal characteristic values.
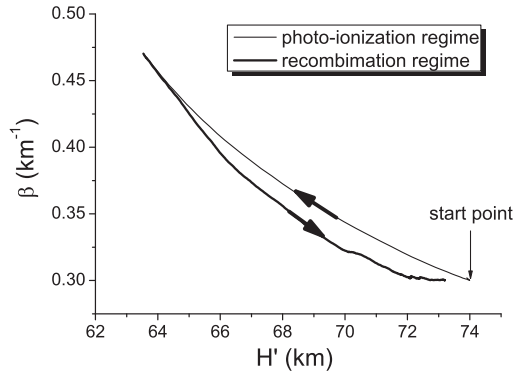
Fig. 3. The connection between ionospheric parameters $H'(t)$ and $\beta(t)$ during photo-ionization and recombination regimes.

Fig. 4). These two time domains are also characterized by the type of the dominant process involving electrons: the photo-ionization in the first domain and recombination processes (electron–ion, ion–ion and three body recombination) in the latter.

The mutual relation of ionospheric parameters $\beta(t)$ and $H'(t)$ is given in Fig. 3 for two time intervals related to the photo-ionization and recombination regime, respectively. The starting point $H'(t) = 74$ km and $\beta(t) = 0.3$ km^{-1} is related to the unperturbed ionosphere before the onset of the considered flare. We see that the curves for the photo-ionization and recombination regime have different profiles meaning that $\beta(t)$ and $H'(t)$ follow different patterns during the two regimes, i.e. they look like hysteresis curves

between the starting and end position. In principle, the curve in Fig. 3 need not be closed as the starting and the end point in the $\beta-H'$ diagram may be related to different unperturbed states. Namely, although the ionosphere is considered unperturbed before the flare onset and after a sufficiently long relaxation time after the disappearance of the flare, these two unperturbed states may not coincide as the unperturbed ionosphere itself is not necessarily stationary and it may have changed within this time interval for various reasons (like the Earth rotation, etc.). According to Fig. 3, it can be concluded that, at a given height $H'(t)$ in the D-region, the parameter $\beta(t)$ is larger during the photo-ionization regime than during the recombination regime later on.

The resulting affect of photo-ionization and recombination processes on electron concentration is shown in Fig. 4 for different times during both regimes. We can see that the influence of solar flare is more pronounced at higher altitudes. At all altitudes, the electron concentration increases in time in the photo-ionization regime while it decreases in the recombination regime. Also, the latter regime lasts longer than the former one.

At higher altitudes, the solar radiation affects more the time and spatial (with respect to h) derivatives of electron concentration as seen in Figs. 5 and 6, respectively. In the photo-ionization regime, the time derivative is positive, it gets smaller and tends to zero near the electron concentration maximum. The negative values are obviously related to the recombination regime when the electron concentration decreases in time tending to become (quasi) stationary. As to the spatial derivative of the electron concentration, the photo-ionization and the recombination regimes exhibit opposite time behaviors: rising and falling in time respectively at all heights h.
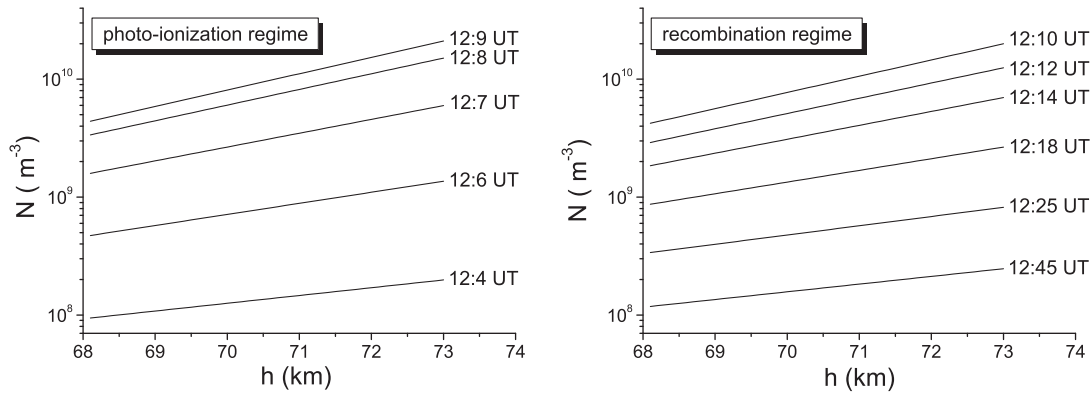

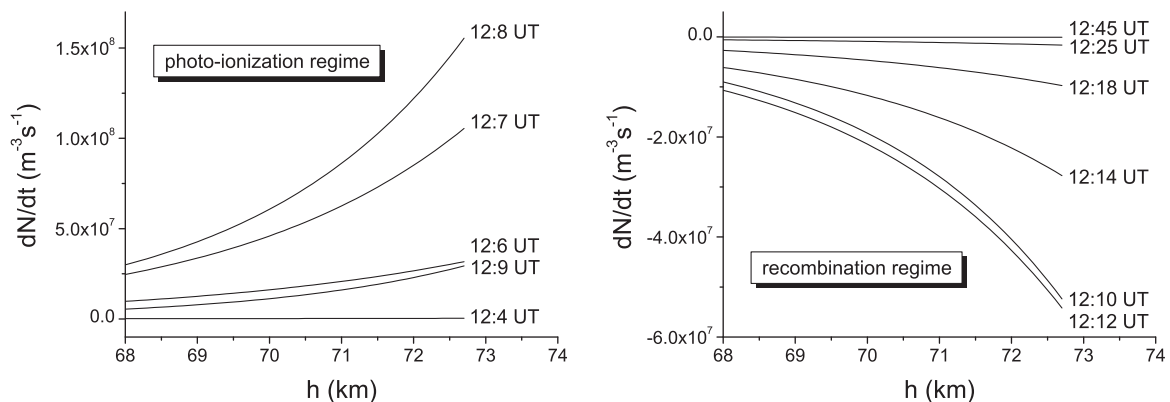**Fig. 4.** The vertical distribution of electron concentration during photo-ionization and recombination regimes.

Fig. 5. The vertical distribution of t-derivative of electron concentration during photo-ionization and recombination regimes.
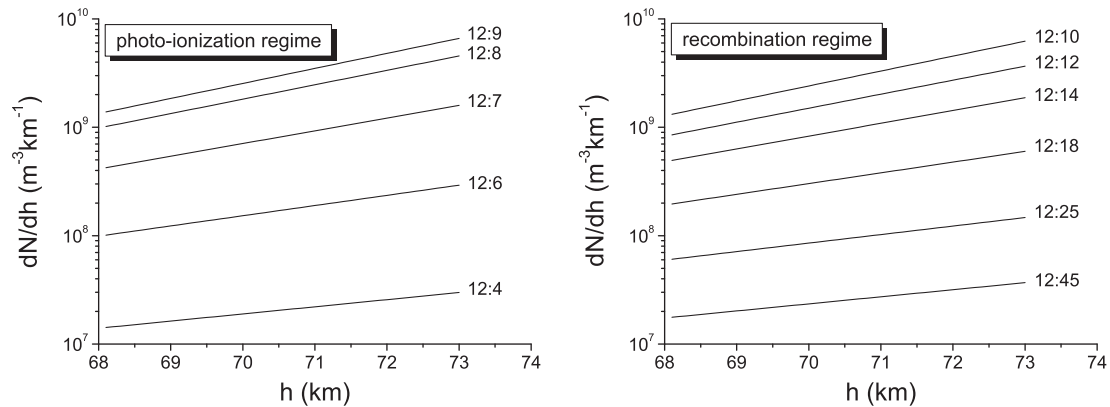
Fig. 6. The vertical distribution of *h*-derivative of electron concentration during photo-ionization and recombination regimes.

4. Conclusion

In this paper, we have presented an analysis on electron concentration variation in the ionospheric D-region during the solar flare of class M1.0 ($I_{max}(t = 12{:}07\ \text{UT}) = 1.06 \times 10^{-5}\ \text{W/m}^2$) that occurred on March 24, 2011. Two ionospheric parameters, the wave reflection high $H'(t)$ and sharpness $\beta(t)$, are obtained by comparing amplitude and phase changes of the signal emitting from the DHO transmitter and recorded by Belgrade receiver station, with correspondent values calculated by the LWPC program. From these parameters, the spatial distribution of electron concentration and its time and height derivatives are calculated.

We have shown that two characteristic regimes show up: the photo-ionization regime where the photo-ionization process dominate, and recombination regime with dominant recombination processes.

In the lower ionosphere, the electron concentration and its spatial gradient increase with height during both regimes. The electron concentration thus starts growing due to photo-ionization processes that prevail after the flare onset, then it reaches a maximum and, soon after the flare maximum, begins falling off due to the prevailing recombination processes.

The spatial derivative of the electron concentration shows to be positive always, e.g. the considered concentration is increasing function of height *h*. The reflection height H' is shifting downwards during the photo-ionization regime and upwards during the recombination regime.

As seen in Fig. 5, the time derivative of the electron concentration is positive and negative in the photo-ionization and recombination process, respectively.

Finally, we see that the solar flare impact on the shape of the electron concentration profile grows with height.

Acknowledgment

References

[1] J.M. Goodman, Adv. Space. Res. 36 (2005) 2241.
[2] S.M. Stankov, N. Jakowski, K. Tsybulya, V. Wilken, Radio Sci. 41 (2006) RS6S09.
[3] M. Hayakawa, Y. Kasahara, T. Nakamura, Y. Hobara, A. Rozhnoi, M. Solovieva, O.A. Molchanov, J. Atm. Sol. Terr. Phys. 72 (2010) 982.
[4] S.M. Radicella, M.L. Zhang, Ann. Geophys. 38 (1995) 35–41.
[5] N.R. Thomson, M.A. Clilverd, C.J. Rodger, J. Geophys. Res. 116 (2011) A03310.
[6] W.M. McRae, N.R. Thomson, J. Atm. Sol. Terr. Phys. 66 (2004) 77.
[7] V. Žigman, D. Grubor, D. Šulić, J. Atm. Sol. Terr. Phys. 69 (2007) 775–792.
[8] J.A. Ferguson, Computer Programs for Assessment of Long-Wavelength Radio Communications, Version 2.0, Space and Naval Warfare Systems Center, San Diego, CA, 1998.
[9] D.P. Grubor, D.M. Šulić, V. Žigman, Ann. Geophys. 26 (2008) 1731.
[10] D. Šulic, A. Nina, V. Sreckovic, Pub. Astro. Obs. Belgr. 89 (2010) 391.
[11] J.R. Wait, K.P. Spies, Characteristics of the Earth-ionosphere waveguide for VLF radio waves, NBS Technical Note, 300, Colorado, 1964.
[12] N.R. Thomson, C.J. Rodger, M.A. Clilverd, J. Geophys. Res. 110 (2005) A06306.